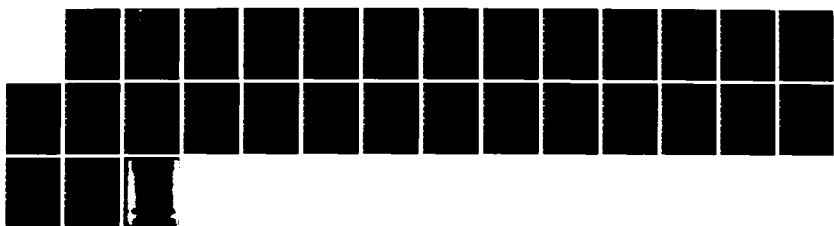


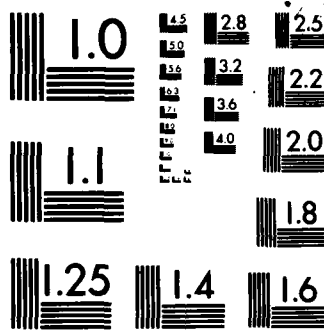
AD-A141 328 ATOMIC COLLISIONS AND PLASMA PHYSICS(U) PITTSBURGH UNIV 1/1
PA DEPT OF PHYSICS AND ASTRONOMY M A BIONDI 31 JAN 84
AFGL-TR-84-0044 F19628-81-K-0002

UNCLASSIFIED

F/G 7/4

NL





MICROCOPY RESOLUTION TEST CHART
NATIONAL BUREAU OF STANDARDS 1963 A

AD-A141 320

REF ID: A6444-0044

ATOMIC COLLISIONS AND PLASMA PHYSICS

Manfred A. Biondi
Department of Physics and Astronomy
University of Pittsburgh
Pittsburgh, Pa. 15260

31 January 1984

Final Report for Period 1 November 1980 - 31 December 1983

Approved for public release; distribution unlimited

This research was supported by the Defense Nuclear Agency under
the Nuclear Weapons Effects Program, Subtask S99QMXBD, Work Unit 09.

DTIC FILE COPY

AIR FORCE GEOPHYSICS LABORATORY
AIR FORCE SYSTEMS COMMAND
UNITED STATES AIR FORCE
HANSOM AFB, MASSACHUSETTS 01731

84 05 17 003

This report has been reviewed by the ESD Public Affairs Office (PA) and is releasable to the National Technical Information Service (NTIS).

This technical report has been reviewed and is approved for publication

John F. Paulson

JOHN F. PAULSON
Contract Manager

Rocco Narcisi

ROCCO S. NARCISI
Branch Chief

FOR THE COMMANDER

Robert A. Skrivaneck

ROBERT A. SKRIVANEK
Acting Division Director

Qualified requestors may obtain additional copies from the Defense Technical Information Center. All others should apply to the National Technical Information Service.

If your address has changed, or if you wish to be removed from the mailing list, or if the addressee is no longer employed by your organization, please notify AFGL/DAA, Hanscom AFB, MA 01731. This will assist us in maintaining a current mailing list.

Do not return copies of this report unless contractual obligations or notices on a specific document requires that it be returned.

UNCLASSIFIED

SECURITY CLASSIFICATION OF THIS PAGE (When Data Entered)

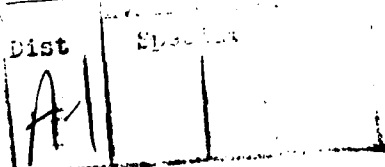
REPORT DOCUMENTATION PAGE		READ INSTRUCTIONS BEFORE COMPLETING FORM
1. REPORT NUMBER AFGL-TR-84-0044	2. GOVT ACCESSION NO. AD-A141320	3. RECIPIENT'S CATALOG NUMBER
4. TITLE (and Subtitle) ATOMIC COLLISIONS AND PLASMA PHYSICS	5. TYPE OF REPORT & PERIOD COVERED Final - 11/1/80 - 12/31/83	
7. AUTHOR(s) Manfred A. Biondi	6. PERFORMING ORG. REPORT NUMBER F19628-81-K-0002	
9. PERFORMING ORGANIZATION NAME AND ADDRESS University of Pittsburgh Pittsburgh, PA 15260	10. PROGRAM ELEMENT, PROJECT, TASK AREA & WORK UNIT NUMBERS AXHDCDAB	
11. CONTROLLING OFFICE NAME AND ADDRESS Air Force Geophysics Laboratory Hanscom AFB, MA 01731 Monitor/John F. Paulson/LID	12. REPORT DATE 31 January 1984	
14. MONITORING AGENCY NAME & ADDRESS (if different from Controlling Office)	13. NUMBER OF PAGES 27	
16. DISTRIBUTION STATEMENT (of this Report)	15. SECURITY CLASS. (of this report) Unclassified	
	15a. DECLASSIFICATION/DOWNGRADING SCHEDULE	
17. DISTRIBUTION STATEMENT (of the abstract entered in Block 20, if different from Report)	NA	
18. SUPPLEMENTARY NOTES This research was supported by the Defense Nuclear Agency under the Nuclear Weapons Effects Program, Subtask S99QMXBD, Work Unit 09.		
19. KEY WORDS (Continue on reverse side if necessary and identify by block number) Ion-molecule reaction rates, electron-ion recombination rates, drift tubes, microwave afterglow apparatus, charge transfer, atom transfer, ion-molecule association, metastable state ions, mobility differentiation, dissociative recombination, O^+ , O_2^+ , O^{++} , O_2^{++} , N^+ , N_2^+ , NO^+ , $CO^+ \cdot CO$, $N_2^+ \cdot N_2$, $O_2^+ \cdot O_2$, electrons, O_2 , N_2 , CO_2 , He, Ne.		
20. ABSTRACT (Continue on reverse side if necessary and identify by block number) Experimental studies have been carried out of ion-molecule interactions and reactions and electron-ion recombination reactions of interest in modelling the normal and disturbed regions of the earth's upper atmosphere. Drift tube and microwave afterglow techniques were employed for these studies. Rates of charge transfer, atom transfer and association in ion-molecule collisions involving both ground-state and metastable-state ions were determined at thermal energies for O^{++} , NO^+ , O_2^+ , N^+ and N_2^+ ions and He, O_2 , N_2 and CO_2 molecules. Mobility		

UNCLASSIFIED

SECURITY CLASSIFICATION OF THIS PAGE(When Data Entered)

20.

differentiation studies for ground state and metastable O^+ , O_2^+ , O^{++} and O_2^{++} ions moving in He or Ne gas were carried out. Recombination rates between electrons and $CO^+ \cdot CO$, $N_2^+ \cdot N_2$ (i.e., N_4^+) and $O_2^+ \cdot O_2$ (i.e., O_4^+) ions were determined over a wide range of electron temperature.



UNCLASSIFIED

SECURITY CLASSIFICATION OF THIS PAGE(When Data Entered)

I. Introduction

During the 3-year period of Contract F19628-81-K-0002, experimental studies of ion-molecule interactions and reactions and of electron-ion recombination were carried out via drift tube and microwave afterglow techniques, respectively.

The ion-molecule interactions and reactions studied included:

- a) thermal energy charge transfer and atom transfer when O^{++} ions in both their ground 3P and metastable 1D and 1S states collide with He, O_2 , N_2 and CO_2 atoms or molecules,
- b) mobility differentiation between ground-state and metastable ions; here O^+ , O_2^+ , O^{++} and O_2^{++} ions moving in helium or in neon gas,
- c) ion-molecule association/dissociation reactions at low temperatures; here the ions were NO^+ , O_2^+ , N^+ and N_2^+ combining in three-body collisions at thermal energies (100 K to 400 K) with N_2 and CO_2 molecules.

The electron-ion recombination studies involved dissociative recombination between electrons and dimer-cluster ions, here $CO^+\cdot CO$ (and $CO^+\cdot (CO)_2$), $N_2^+\cdot N_2$ and $O_2^+\cdot O_2$. The recombination coefficient was determined over a wide range of electron temperatures (ambient thermal to ~ 7000 K).

The detailed descriptions of the methods of study, experimental measurements, results and conclusions for these various topics are given in papers published or to be published which are described in Sections II and III and the Appendix.

II. Research Published during the Present Contract

The texts of each of the following papers appears in the Appendix of this report.

A. Ion-Molecule Reactions

1. "Reactions of ground-state and metastable O^{++} ions with He,

O_2 , N_2 and CO_2 at thermal energies", R. Johnsen and M. A. Biondi.

2. "Mobilities of ground-state and metastable O^+ , O_2^+ , O^{2+} and O_2^{2+} ions in helium and neon", Rainer Johnsen, Manfred A. Biondi and Makoto Hayashi.
3. "Laboratory measurements of the association rate coefficients of NO^+ , O_2^+ , N^+ , and N_2^+ ions with N_2 and CO_2 at temperatures between 100 K and 400 K", Seksan Dheandhanoo and Rainer Johnsen.

B. Electron-Ion Recombination

1. "Electron-temperature dependence of dissociative recombination of electrons with $CO^+ \cdot (CO)_n$ -series ions", Marlin Whitaker, Manfred A. Biondi and Rainer Johnsen.
2. "Electron-temperature dependence of dissociative recombination of electrons with $N_2^+ \cdot N_2$ dimer ions", Marlin Whitaker, Manfred A. Biondi and Rainer Johnsen.

III. Research Results to be Readied for Publication

A. Recombination of O_4^+ Ions with Electrons as a Function of T_e

Using microwave afterglow techniques similar to those described in Sec. II B. 1 and 2 the variation of the recombination coefficient $\alpha(O_4^+)$ with electron temperature T_e has been determined over the range $140 K \leq T_e \leq 7600 K$ and $T_+ = T_n = 140 K$. The results of the studies may be expressed in the form

$$\alpha(O_4^+) = (3.9 \pm 0.4) \times 10^{-6} [T_e(K)/300]^{-0.55} \text{ cm}^3/\text{s} .$$

Thus the behavior of the dimer ion $O_2^+ \cdot O_2$ (i.e., O_4^+) is similar to that observed for $CO^+ \cdot CO$ and $N_2^+ \cdot N_2$ (i.e., N_4^+) ions - a large coefficient

at 300 K ($> 10^{-6}$ cm³/sec) and a variation close to $T_e^{-1/2}$. These results will be readied for publication as part of our ongoing work.

Appendix

Texts of papers published in scientific journals during the period of this contract are given on the following pages.

Reactions of ground-state and metastable O^{2+} ions with He, O_2 , N_2 , and CO_2 at thermal energies

Rainer Johnsen and Manfred A. Biondi

Department of Physics and Astronomy, University of Pittsburgh, Pittsburgh, Pennsylvania 15260
(Received 16 July 1980; accepted 10 September 1980)

Evidence is presented that some previous studies of reactions of O^{2+} ions with various atoms and molecules referred to ion samples composed in part of ions in metastable (1D and/or 1S) states. This finding resolves the 3 orders of magnitude discrepancy between previous experimental and calculated rate coefficients for the $O^{2+}(^1P) + He$ charge transfer process. Using a drift tube to distinguish, via arrival time differences, ground-state $O^{2+}(^3P)$ and metastable ions, a rate coefficient of $(3.5 \pm 1.5) \times 10^{-11} \text{ cm}^3/\text{sec}$ is obtained for the reaction, in good agreement with that obtained from *ab initio* theoretical calculations. Previous conclusions concerning reactions of O^{2+} with O_2 and N_2 , however, remain valid since the difference in reactivity of ground-state and metastable O^{2+} ions appears to be negligible in this case. The rate coefficient for the reaction $O^{2+} + CO_2$ has been determined to be $(2 \pm 0.5) \times 10^{-9} \text{ cm}^3/\text{sec}$ for ions either in the ground-state or in metastable states.

I. INTRODUCTION

The recent observation of doubly charged oxygen ions in the earth's ionosphere and proposed photochemical models involving such ions¹ have motivated several studies^{2,3} of reactions of O^{2+} ions with atmospheric constituents, most importantly O_2 and N_2 . These measurements indicated that the destruction of O^{2+} ions in reactions with N_2 would be considerably faster than the photochemical model had assumed, a finding which has led to a search for additional sources of O^{2+} ions.⁴

In another context, Dalgarno *et al.*⁵ performed theoretical calculations of the charge transfer of O^{2+} ions with helium and found a moderate rate coefficient for the process, $k \approx 2 \times 10^{-11} \text{ cm}^3/\text{sec}$, at temperatures near 1000°K. Since this result was in sharp contrast to the very small value, $\sim 10^{-14} \text{ cm}^3/\text{sec}$, inferred in the experiment of Howorka *et al.*,³ Dalgarno *et al.* introduced adjustments to the theoretically calculated interaction parameter to obtain agreement with experiment. Such a large adjustment of the theoretical value seems unsatisfactory and by implication casts doubt on the validity of calculated charge transfer coefficients. It appeared worthwhile, therefore to investigate alternate possibilities of reconciling theory and experiment.

Experience gained in studies of doubly charged rare gas ions⁶ suggested that the experimental measurements of Howorka *et al.*³ might refer to O^{2+} ions in an excited state, invalidating a comparison with theoretical calculations for ground state ions. As described below, we have obtained experimental evidence to support this hypothesis and conclude that the theoretical value for the $O^{2+}(^3P) - He$ charge transfer rate is correct. Further, since the previous experimental measurements^{2,3} were carried out with O^{2+} ions that were either partly or completely in metastable states, the measured reaction rates might not be applicable to ionospheric models. (Fortunately, our measurements indicate that charge transfer with molecules (O_2 , N_2) is insensitive to the particular state of the O^{2+} ion.) Finally, the reaction of O^{2+} ions with CO_2 was included in this study because of its possible importance in the ionospheres of the inner, CO_2 -rich planets.

II. EXPERIMENTAL METHOD AND MEASUREMENTS

Our drift-tube mass-spectrometer apparatus and the essential features of the experimental techniques were the same as used in our previous study of the $O^{2+} + O_2$ and $O^{2+} + N_2$ reactions.² Again, the minor branch (< 10%) of the reaction of Ne^{2+} ions with O_2 molecules was used as a source of O^{2+} ions, i.e.,



Since the original work was carried out, the efficiency of the ion detection system has been improved significantly, so that, in a neon carrier gas with small additions of O_2 (typically $\sim 3 \times 10^{-5}$ Torr of O_2 in 0.5 Torr of neon), it is possible to analyze the detailed structure of the O^{2+} arrival spectra produced by the reaction. It was found that the three low-lying states of Ne^{2+} (i.e., the 3P ground state and the 1D and 1S metastable states), which are distinguishable by their different ionic mobilities,⁷ each contribute to the observed O^{2+} arrival spectrum with comparable efficiencies (the 1D state is $\sim 3 \times$ more effective than the 3P ground state).

An example of an O^{2+} arrival spectrum is shown in Fig. 1(b), with its decomposition into components arising from the different Ne^{2+} states [shown in Fig. 1(a)]. (Since, in neon, O^{2+} ions have a higher mobility than do Ne^{2+} ions, an O^{2+} component formed from a particular Ne^{2+} state exhibits an arrival spectrum extending from the transit time across the drift region of that Ne^{2+} state to an earlier time corresponding to the O^{2+} transit time.) Also shown, in Fig. 1(c), is an arrival spectrum recorded when a small amount of helium (5×10^{-3} Torr) was added to the neon carrier gas. It is clear that only one component of the O^{2+} arrival spectrum, the one due to $Ne^{2+}(^3P)$, was affected by the addition of helium, indicating that it is composed of O^{2+} ions in a different state than the others. Based on theoretical arguments (see Sec. III) this finding suggests identification of this group as $O^{2+}(^3P)$, while the other O^{2+} ions should be in metastable states (1D and/or 1S).

The preferential loss of the leading edge of the $O^{2+}(^3P)$ arrival spectrum occurs because those O^{2+} ions were produced at early times (near the drift tube entrance)

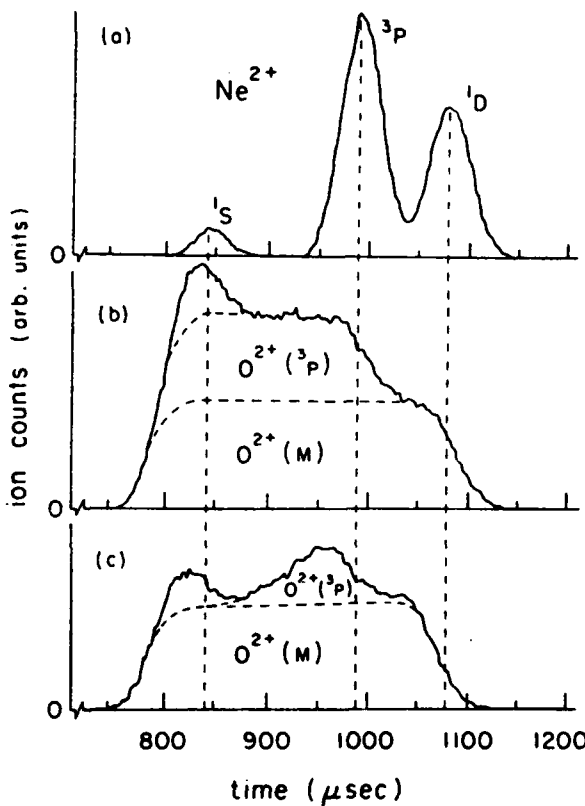


FIG. 1. Examples of Ne^{2+} parent ion and O^{2+} product ion arrival spectra: (a) Ne^{2+} ions in the indicated states, (b) O^{2+} ions' spectrum without addition of helium and (c) with helium added. The O^{2+} arrival spectra are interpreted as superpositions of three components, each extending from the transit time of O^{2+} to that of the Ne^{2+} parent ion. Conditions: $p(Ne) = 0.54$ Torr, $p(O_2) \sim 10^{-3}$ Torr, $p(He) = 0$ (part b) and 5×10^{-3} Torr (part c); $E/N = 20$ Td.

and, having traversed a greater distance from their point of creation to the drift tube's exit, have suffered a larger loss in reactions with helium. This effect can be used to obtain semiquantitative values for the rate coefficient of the single-electron charge-transfer reaction



Of the products of Reaction (2) only He^+ was observable, while the O^+ product was obscured completely by the larger signal from the charge transfer reaction $Ne^{2+} + O_2$. Also, the reaction of Ne^{2+} with helium is fortunately extremely slow,⁷ so that its He^+ product ions, while observable, were not confused with those of Reaction (2).

Similar data to those shown in Fig. 1 were taken at several helium densities and yielded rate coefficients between 2×10^{-11} and 5×10^{-11} cm³/sec for Reaction (2). The uncertainty in this value is largely due to the difficulty of accurately decomposing the O^{2+} arrival spectra, a problem which, in principle, could be overcome by computer-fitting procedures. The majority of data were taken at sufficiently low values of E/N (the electric field

to gas-density ratio) that the O^{2+} ions' mean energy was raised only slightly above ambient (to ~ 400 °K). Some data were taken at higher drift fields where the different states of Ne^{2+} are no longer distinguishable by differences in ionic mobilities. It was still possible, however, to obtain estimates for the rate coefficient of Reaction (2) at effective temperatures of the O^{2+} ions near 1000 °K. The values were similar to those obtained at the lower temperatures (i.e., between 2×10^{-11} and 5×10^{-11} cm³/sec). Obviously, the large uncertainties in the values precluded determination of the temperature dependence of Reaction (2).

Rate coefficients for the reactions of O^{2+} with O_2 and N_2 had been determined in our previous experiments²; however, the presence of several distinguishable states of O^{2+} was not appreciated at that time. In the course of the present experiments, a search was made for possible differences in the rate coefficients for ground-state and metastable-state O^{2+} ions reacting with O_2 , N_2 , and CO_2 . No such effects were found. It appears that both ground-state and metastable O^{2+} ions react with the molecular gases mentioned above with essentially the same rate coefficients. Differences in reactivity of about 20% should have been detectable but were not found.

The rate coefficient for the $O^{2+} + CO_2$ reaction was measured and found to have a value of $(2 \pm 0.5) \times 10^{-9}$ cm³/sec at an effective temperature of ~ 400 °K. It was not possible to determine the product ions of this reaction, since in all cases the expected products are more abundantly produced by the reaction of the unavoidably present Ne^{2+} with CO_2 .

III. DISCUSSION OF RESULTS AND CONCLUSIONS

The experimental results indicate only that two (or more) different states of O^{2+} were present in the studies; the identification of these states by experimental means, as is often the case, is difficult, but the theoretical calculations of Dalgarno *et al.*⁵ clearly suggest that the state which reacts with helium is the 3P ground state of O^{2+} . Other possible identifications would be 1D or 1S , of which the 1D state can probably be ruled out on theoretical grounds, since Dalgarno *et al.*⁶ have extended their calculations to the reaction of $O^{2+}(^1D) + He$ and find that the reaction should be negligibly slow at near-thermal energies. The identification of the O^{2+} state as 1S seems equally unlikely; formation of $O^+(^1P)$ ions in the process $O^{2+}(^1S) + He - O^+(^1P) + He^+(^1S)$ should be the favored exit channel for the reaction, but the small exoergicity of the process (about 1 eV) would lead to a potential curve crossing between initial and final states at internuclear separations $\sim 1.5 \times 10^{-7}$ cm, too large for efficient charge transfer. Indeed, similar reactions⁶ between doubly charged rare gas ions and rare gas atoms have invariably been found to be slow when the exoergicity was less than about 2 eV. By contrast, the reaction $O^{2+}(^1S) + Ne - O^+(^1P) + Ne^+(^2P)$ is exoergic by almost exactly 4 eV, which has been found to be the optimal value for charge transfer.⁶ Thus, even if the 1S state is produced in our experiments, it should be eliminated very quickly in reactions with the abundant carrier gas neon. We therefore conclude that the state

which reacts with helium is O^{2*}(³P).

The measured rate coefficient for O^{2*}(³P) + He, $k = (3.5 \pm 1.5) \times 10^{-11}$ cm³/sec, agrees within a factor of two with the theoretical value of Dalgarno *et al.*,⁵ which is quite good, in view of the uncertainties in both the theoretical treatment and the experimental determination. The results presented here also imply that the measurements by Howorka *et al.*,³ carried out in high-density helium carrier gas, refer to O^{2*} ion samples depleted of all ground-state ions and hence to O^{2*} ions in a mixture of the ¹D and ¹S states. As noted earlier, the measurements by Johnsen and Biondi² referred to a mixture of ground-state and metastable ions rather than, as was then believed, to ground state ions. However, the conclusions drawn from these measurements concerning applications to ionospheric models remain valid. Reactions with N₂ and O₂ are fast for both ground-state and metastable O^{2*} ions; thus the problem of accounting for the substantial O^{2*} concentrations observed in the *F*-region remains.

ACKNOWLEDGMENTS

This research was supported, in part, by the NASA Planetary Atmospheres Program under Grant No. NGL39-011-137 and the Army Research Office/DNA under Grant No. DAAG29-79-C-0043.

- ¹E. L. Breig, M. R. Torr, D. G. Torr, W. B. Hanson, J. H. Hoffman, J. C. G. Walker, and A. O. Nier, *J. Geophys. Res.* 82, 1008 (1977).
- ²R. Johnsen and M. A. Biondi, *Geophys. Res. Lett.* 5, 847 (1978).
- ³F. Howorka, A. A. Viggiano, D. L. Albritton, E. E. Ferguson, and F. C. Fehsenfeld, *J. Geophys. Res.* 84, 5941 (1979).
- ⁴G. A. Victor and E. R. Constantines, *Geophys. Res. Lett.* 6, 519 (1979).
- ⁵A. Dalgarno, S. E. Busler, and T. G. Heil, *J. Geophys. Res.* 2 (1980).
- ⁶R. Johnsen and M. A. Biondi, *Phys. Rev. A* 20, 87 (1979).
- ⁷R. Johnsen and M. A. Biondi, *Phys. Rev. A* 18, 996 (1978).
- ⁸A. Dalgarno (private communication).

Mobilities of ground-state and metastable O^+ , O_2^+ , O^{2+} , and O_2^{2+} ions in helium and neon

Rainer Johnsen, Manfred A. Biondi, and Makoto Hayashi^{a)}

Department of Physics and Astronomy, University of Pittsburgh, Pittsburgh, Pennsylvania 15260
(Received 4 May 1982; accepted 12 May 1982)

The ionic mobilities of O^+ , O_2^+ , O^{2+} , and O_2^{2+} in helium and neon have been measured using a selected-ion drift apparatus (SIDA). It is found that the mobilities of both O^+ and O_2^+ ions in the metastable states (3D or 3P) are measurably smaller than those of the same ions in their ground states. The detection and identification of metastable ions was carried out by using known, state-selective ion-molecule reactions. A similar mobility differentiation of ground-state and metastable ions was not observed for the O^{2+} and O_2^{2+} ions.

I. INTRODUCTION

Two recent experimental studies^{1,2} of the reactivity of metastable $O^+({}^3D)$ ions made use of the fact that the metastable fraction of the O^+ ion sample could be readily distinguished from that in the ground state by exploiting a small difference in the ionic mobilities of the two ions in helium gas. The utility of state-specific mobilities in studies of low-energy ion-molecule reactions is obvious, but available mobility data suggest that, in general, ionic mobilities depend very little on the internal state of the ion unless symmetry effects are important. The abovementioned case of O^+ ions in helium was the only example in which state-specific mobilities were observed for ions drifting in a chemically different gas.

In an attempt to find additional examples of state-dependent mobilities, we have examined the mobilities of molecular and atomic oxygen ions, both singly and doubly charged, in the gases helium and neon. Several of these ions are known to possess metastable states, and ion-molecule reactions are known that can be used to identify the particular states. Helium and neon were chosen as the neutral atoms since, because of their small electrical polarizabilities, the ion-atom interaction is not dominated by the long-range polarization force, which leads to mobilities which are not state specific.

II. APPARATUS AND EXPERIMENTAL METHOD

The measurements were carried out in the selected ion drift apparatus (SIDA) shown schematically in Fig. 1. The drift tube proper, the mass filter used for ion analysis and the associated electronic equipment were the same as used in a simpler version of the apparatus³ which has been described several times. An additional vacuum chamber was added which contained the electron impact ion source and a quadrupole mass filter to select ions of the desired mass-to-charge ratio from among those produced in the ion source. This arrangement, primarily intended for ion-molecule reaction studies, was also found to be advantageous in studies of ion mobilities.

The U.S. Government is authorized to reproduce and sell this report. Permission for further reproduction by others must be obtained from the copyright owner.

^{a)}Nagoya Institute of Technology, Gokiso-cho, Showa-ku, Nagoya, Japan.

Under typical operating conditions, a mass-selected pulse of ions (containing $\sim 10^5$ ions) is injected into the drift region with an energy of about 10 eV and at a repetition rate of $\sim 10^3$ Hz. Following thermalization through collisions with the neutral gas atoms, the ion cloud traverses the drift tube with a drift velocity appropriate to the ionic mobility, applied electric field and gas density. Those ions effusing through the exit orifice of the drift region (approximately one ion of the 10^5 injected per pulse) are mass analyzed and detected by a particle detector (channel electron multiplier). Ion counts are accumulated in a multichannel analyzer operated in a time-of-flight mode. The mean transit time of ions through the drift tube is then found from the distribution of counts stored in the multichannel analyzer after applying a correction for the brief times of traversal of the mass spectrometers. As is customary, the measured mobilities have been reduced to a standard density of $2.69 \times 10^{19} \text{ cm}^{-3}$ and are given as a function of the electric field to neutral gas density ratio E/N in units of Td ($1 \text{ Td} = 10^{-17} \text{ V cm}^2$).

The experimental uncertainties arising from inaccuracies in voltage and pressure measurements are $\lesssim 1\%$. A larger source of error, unavoidable in this type of apparatus, is associated with the injection of ions into the drift cell at an energy considerably in excess of the final drift energy. This "injection effect" leads to an erroneously large value for the mobilities measured at lower gas pressures (an error of $\sim 5\%$ at a pressure of 0.25 Torr, compared to $\sim 1\%$ at 1 Torr). Therefore, where necessary, the data were corrected by corresponding amounts. In order to test the accuracy of the data, the mobility of Ne^+ ions in neon was measured and compared with the values obtained by Helm⁴; the agreement was better than 2% .

III. MEASUREMENTS

A. Mobilities of oxygen ions of $m/q = 16$ in helium

At low values of E/N , three groups of oxygen ions with a mass-to-charge ratio $m/q = 16$ could be distinguished by their different mobilities in helium. An example of a recorded arrival-time spectrum is given in Fig. 2, which is typical of the data obtained at low E/N and pressures near 1 Torr. It is clear that the intensities of the three groups of ions are comparable and

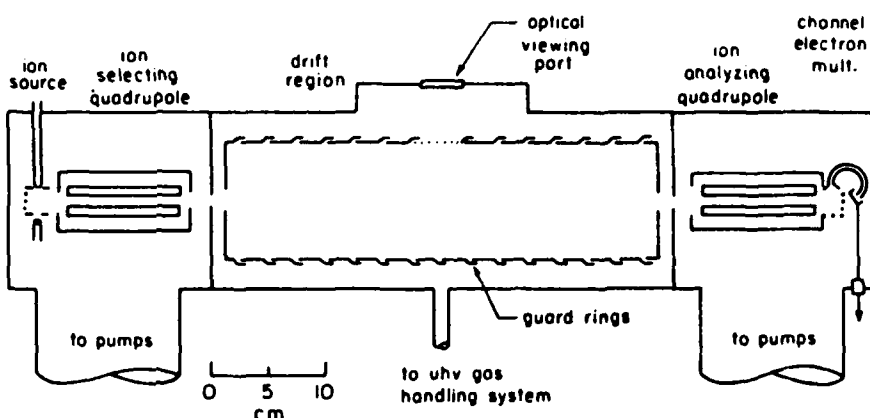


FIG. 1. Schematic diagram of the selected ion drift apparatus (SIDA).

that the assumption of a purely ground-state O^+ ion sample would be erroneous. The identification of the two ions of higher mobilities has been discussed in detail previously^{1,2}; the fastest ion is evidently $O^+(^4S)$, while the ion with the next highest mobility has been identified as metastable $O^+(^2D)$, with a possible admixture of $O^+(^2P)$.

The third ion group (lowest mobility) was found to have a significantly higher appearance potential than the other two ions. The suspicion that this ion was O_2^{2+} rather than another metastable state of O^+ was confirmed by tests in which the reactivity of this ion with other gases was investigated. When traces of N_2 were added to the helium, the ion was rapidly converted into two ions N_2^+ and O_2^+ (with a rate coefficient of $2 \times 10^{-9} \text{ cm}^3/\text{s}$). Similarly, when neon was added to the helium, both Ne^+ ions and O_2^+ ions were produced. Both observations are consistent with single charge transfer from an initial, *doubly* charged ion. According to the calculations by Hurley⁵ of the $O_2^{2+}(^1\Sigma_g)$ potential energy curves, single charge transfer of this ion with neon would be nearly energy resonant, which is generally not sufficient for low-energy charge transfer from doubly charged ions. It seems likely, though, that the O_2^{2+} ion is formed by vertical ionization into a vibrationally excited state with $v=5$, in which case charge transfer with neon would be exoergic by about 2 eV. It

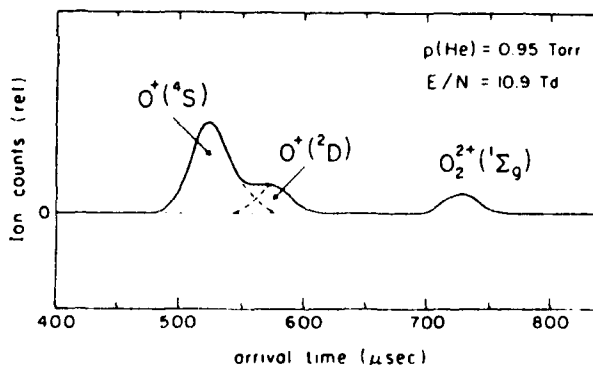


FIG. 2. Example of an arrival-time spectrum of $m/q = 16$ amu ions in helium gas at $p(\text{He}) = 0.95$ Torr, $E/N = 10.9$ Td, and drift region length = 35.66 cm.

is therefore concluded that the ion of lowest mobility is $O_2^{2+}(^1\Sigma_g)$, possibly with vibrational excitation near $v=5$.

The measured mobilities in helium are shown in the uppermost portion of Fig. 3. Above $E/N = 40$ it was not possible to resolve the different groups of ions; thus no attempt was made to distinguish the ion mobilities at higher E/N . Data over a larger range of E/N for $O^+(^2D)$ have been obtained by Rowe *et al.*² using a different method described by those authors.

B. Mobilities of oxygen ions of $m/q = 32$ in helium

Mobilities of O_2^+ ions in helium have been measured previously.⁶ From experiments⁶ in which both ground-

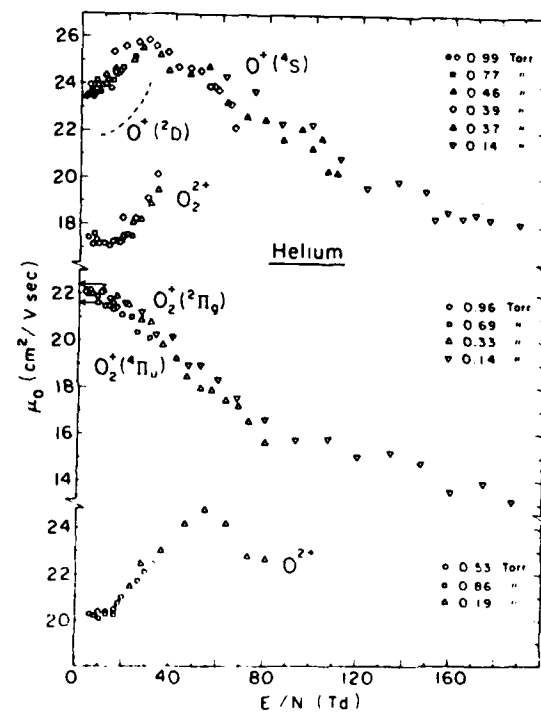


FIG. 3. Measured reduced mobilities of singly and doubly charged oxygen ions in helium as a function of E/N at a gas temperature of 300 K.

state and metastable ($^4\Pi_u$) O_2^+ ions were known to be present, it was concluded that the mobilities of the two ions were nearly the same. The present experiments confirm the finding that the difference in mobilities is indeed very small, but under suitable conditions (pressures near 2 Torr and low E/N) a slight splitting of the O_2^+ arrival peaks is detectable, as indicated in the middle portion of Fig. 3 by the arrows.

$O_2^+ ({}^4\Pi_u)$ ions are known⁶ to undergo a charge transfer reaction with argon which is not energetically possible for O_2^+ ground-state ions. By adding small amounts of argon to the helium it was found that the slower group of O_2^+ ions reacted with argon and hence contained the metastable fraction of the O_2^+ ion samples. While the dependence of ionic mobilities on gas temperature was not the subject of this study, a limited number of measurements were carried out in a smaller, low temperature drift tube at 77 K. It was noted that the splitting of the O_2^+ arrival spectrum into two distinct components was larger than at room temperature.

C. Mobilities of oxygen ions of $m/q=8$ in helium

Although the yield of O_2^{2+} ions produced by electron impact on O_2 was very small (less than 0.1% of that of O^+), for mobility measurements this method of generating O_2^{2+} was found preferable to the indirect method⁷ via the $Ne^{2+} + O_2$ reaction used previously. It is also known from previous work⁷ that ground state O_2^{2+} ions undergo charge transfer with helium; consequently the mobility of these ions in helium cannot be determined. The O_2^{2+} ions observed in the present experiment were therefore expected to be in either or both of the low lying 1D and 1S metastable states.

No splitting of the observed O_2^{2+} arrival spectra into distinguishable components was observed, which may indicate either that only a single metastable state was present or that both states, 1D and 1S , yield the same mobilities in helium. The mobility of O_2^{2+} ions in helium (see the lower portion of Fig. 3) shows a pronounced maximum at E/N values near 55 Td, indicating a weakly attractive potential between O_2^{2+} and He. Because of the low intensity of this ion, it was not possible to extend the measurements to significantly higher E/N .

D. Mobilities of oxygen ions of $m/q=16$ in neon

Two readily distinguishable groups of $m/q=16$ ions were found in neon. Reactivity tests similar to those performed in helium to identify the ion groups were also made in neon. As in helium, the slower of the two O^+ ions reacted rapidly with both N_2 and O_2 by charge transfer, suggesting a metastable O^+ ion, most probably the 2D state ion. The faster group of ions was found to react slowly with O_2 and N_2 , which is typical of O^+ ions in the 4S ground state. The ion O_2^{2+} was not observed in neon, since, as noted in Sec. III A, O_2^{2+} ions are rapidly destroyed by charge transfer with neon. Compared to measurements in helium, the separability of the two O^+ ion groups in neon was considerably better, making neon the gas of choice for measurements where separation of the two ions is desired. The measured mobilities are shown in the uppermost portion of Fig. 4.

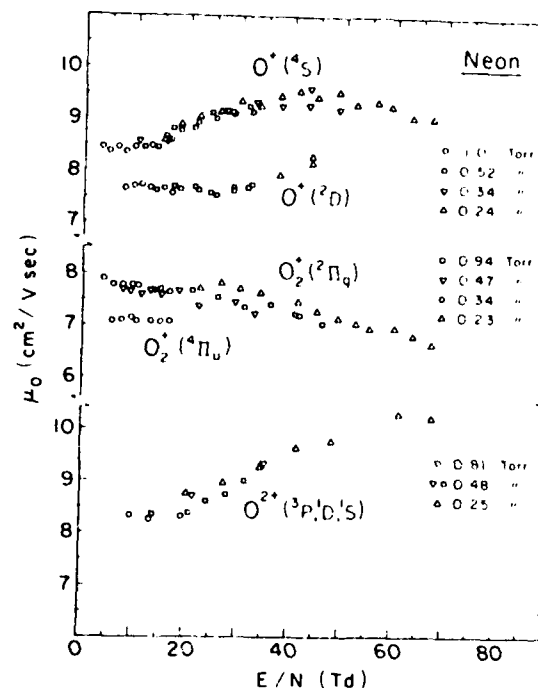


FIG. 4. Measured reduced mobilities of singly and doubly charged oxygen ions in neon as a function of E/N at 300 K.

E. Mobilities of oxygen ions of $m/q=32$ in neon

The arrival time spectra of O_2^+ ions in neon showed a clear splitting into two components of comparable intensity. The ions in the group of lower mobility were found to undergo a charge transfer reaction with argon which is typical of O_2^+ ions in the ${}^4\Pi_u$ metastable state, suggesting this as the most likely identification. The ion group of higher mobility did not react with argon, suggesting that this group contains only O_2^+ ions in the ground state. At E/N values above ~20 Td, the distinguishability of the two ion groups was poor; consequently the average mobility of the mixed ion sample was measured (see middle portion of Fig. 4).

F. Mobilities of oxygen ions of $m/q=8$ in neon

While the arrival time spectra did not give any indication of the presence of more than one state of the O_2^{2+} ion, tests showed that only a portion of the ion population reacted with helium by charge transfer. This reaction, ascribed to $O_2^{2+} ({}^3P)$ ground-state ions, has been studied recently.⁷ These results suggest that at least two states of O_2^{2+} are produced by electron impact on O_2 but that the ionic mobilities of the ions in different states are very nearly identical. The results of the measurements are shown in the lower portion of Fig. 4.

IV. DISCUSSION OF RESULTS

The experimental data presented in the preceding section indicate that the selection of excited states of ions through mobility differentiation may be feasible in more cases than previously thought. This effect can be exploited in measurements of ion-molecule reaction

rates where the presence of metastable ions is often a disturbing factor or where reactions of metastable species are under investigation. The results certainly should not be generalized; in a number of cases ground-state and metastable ions have nearly identical mobilities; therefore, the absence of an observable mobility difference does not imply the absence of metastable ions.

On the basis of available data, mobility differentiation among different states of ions seems to be most pronounced in the light rare gases helium and neon. In the more polarizable, heavier rare gases the dominant ion-neutral interaction at low collision energies arises from the dipole moment induced in the neutral atom; therefore the mobility should depend very little on the internal excitation state of the ion. In support of this hypothesis, in the heavier rare gases various ions of very different chemical nature exhibit mobilities which depend solely on the polarizability of the atom

and the reduced mass of the ion-atom pair, as predicted by the Langevin formula.⁸

ACKNOWLEDGMENT

This research was supported, in part, by Air Force Cambridge/DNA under Grant No. F19628-81-K-002.

- ¹R. Johnsen and M. A. Biondi, *J. Chem. Phys.* **73**, 190 (1980).
- ²B. R. Rowe, D. W. Fahey, F. C. Fehsenfeld, and D. L. Albritton, *J. Chem. Phys.* **73**, 194 (1980).
- ³R. Johnsen and M. A. Biondi, *J. Chem. Phys.* **59**, 3504 (1973).
- ⁴H. Helm, *Chem. Phys. Lett.* **36**, 97 (1975).
- ⁵A. C. Hurley, *J. Mol. Spectrosc.* **9**, 18 (1962).
- ⁶W. Lindinger, D. L. Albritton, M. McFarland, F. C. Fehsenfeld, A. L. Schmeltekopf, and E. E. Ferguson, *J. Chem. Phys.* **62**, 4101 (1975).
- ⁷R. Johnsen and M. A. Biondi, *J. Chem. Phys.* **74**, 305 (1981).
- ⁸P. Langevin, *Ann. Chim. Phys.* **5**, 245 (1905).

SHORT PAPER

LABORATORY MEASUREMENTS OF THE ASSOCIATION RATE COEFFICIENTS OF NO^+ , O_2^+ , N^+ , AND N_2^+ IONS WITH N_2 AND CO_2 AT TEMPERATURES BETWEEN 100 K AND 400 K

Seksan Dheandhanoo and Rainer Johnsen

Department of Physics and Astronomy
 University of Pittsburgh
 Pittsburgh, PA

(Received 31 March 1983)

ABSTRACT

Rate coefficients for the association reactions of NO^+ ions with N_2 and CO_2 , O_2^+ with N_2 , and N^+ and N_2^+ with N_2 have been determined as a function of gas temperature in a laboratory experiment employing a variable-temperature drift-tube apparatus. The measured rate coefficients were fitted to power laws of the form $k = C (T/300)^x$ where the exponents x ranged from 2.2 to 4.3. The strong temperature dependence observed in the case of the reaction of NO^+ with N_2 ($x = 4.3$) supports the thesis by Arnold et al. (1979) that the temperature variability of D-region ion densities is a result of this reaction step in the ion clustering sequence.

1. INTRODUCTION

It has been recognized for some time that three-body association reactions of ions with atmospheric gases provide the principal mechanism by which the primary ions in the D-region are converted to the hydrated ion species observed by rocket borne mass spectrometers. The variability of total ion content and ion density profiles in the D-region has been ascribed (Arnold et al. 1979) to the effect of ambient gas temperature on three-body association reactions, which is particularly strong in the case of reactions leading to weakly bound cluster ions. Laboratory measurements of such reaction coefficients are thus naturally of interest for model calculations of the D-region ion chemistry.

While experimental techniques to study ion-molecule reactions are very well developed, several complications arise in measurements involving weakly bound cluster ions. Unless precautions are taken, such as working at low gas temperatures and providing "scavenger" molecules to prevent the re-dissociation of the product ion clusters, the resulting rate coefficients can be seriously in error. The measurements described below were carried out in a variable-temperature drift-tube mass-spectrometer, which was specifically constructed for such measurements, and the known complicating effects were taken into account. The rate coefficients were measured under strictly thermal equilibrium conditions at temperatures close to those encountered in the D-region. Nitrogen was used as the carrier gas rather than the frequently used helium in order to provide more realistic conditions.

The reactions of N^+ and N_2^+ ions with N_2 are probably not of importance in the D-region but they were studied for comparison with other experimental data and because of their intrinsic interest as basic reactions. The possible role of reactions of ions with neutral, van der Waals dimers will be discussed briefly since such reactions have recently been proposed as alternative reaction paths in both the D-region and laboratory measurements (Calo and Narcisi 1980).

2. EXPERIMENTAL METHOD AND APPARATUS

The variable-temperature drift-tube apparatus used in this work has been described in detail previously (Johnsen et al. 1979).

As in earlier measurements of other reactions, short pulses of parent ions (NO^+ , O_2^+ , etc.) were injected into a drift-reaction chamber containing the reactant gases under study. By application of suitably programmed electric drift fields the ions were transported to the center of the drift chamber, at which time the electric field was turned off and the ions were allowed to react for a variable length of time. Upon restoration of the drift field the ions traversed the remaining part of the drift chamber and representative samples of the ion population were withdrawn from the chamber through a small sampling orifice for subsequent mass analysis and detection. The reaction rates were then obtained from the observed decrease

of the parent ion's number density with increasing reaction time. Corrections were applied to take into account losses of ions by lateral diffusion to the chamber walls.

The gas temperature was adjusted by flowing liquid nitrogen through a cooling jacket surrounding the chamber or heating the chamber by means of electric heaters. All measurements described in this article were made under conditions where the electric drift field was absent during the reaction time. Consequently, the question of ionic velocity distributions in the presence of electric fields did not arise in this work.

In order to measure the forward rate coefficient of the association reactions it was found necessary to inhibit thermal redissociation of the weakly bound cluster ions by converting them into more stably bound cluster ions. An application of this "scavenging" technique to the reaction of NO^+ in N_2 and an analysis of the pertinent rate equations have been described earlier (Johnsen et al. 1975). In addition to estimating the permissible concentrations of scavenging molecules from the rate equations experimental tests were made to ensure that the scavenger concentration was sufficiently large to prevent redissociation of the primary reaction products without introducing additional unwanted reaction paths.

Because of their small binding energies cluster ions are susceptible to fragmentation by collisions with residual gas molecules in the transfer space between the drift chamber and the mass spectrometer. Unless this effect is taken into account, the resulting fragment ions will contribute to the parent ion signal entering the mass spectrometer from the drift chamber and one would obtain erroneously small decay rates of the parent ion. Fortunately, the transit times of clustered and unclustered parent ions were found to be sufficiently different such that this "false" parent ion signal could be subtracted from the observed signal. Conditions were avoided where this separation of the two parts of the parent ion signal was not possible with adequate accuracy.

3. MEASUREMENTS AND RESULTS

A. $\text{NO}^+ + 2\text{N}_2$

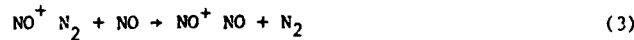
Reactive equilibrium between the association reaction



and its inverse reaction, thermal dissociation



was prevented in these measurements by adding about 2% nitric oxide to the nitrogen. In this case the switching reaction



converted the $\text{NO}^+ \text{N}_2$ ions into the more stable $\text{NO}^+ \text{NO}$ ions at a much higher rate than that of reaction (2) and the decline of the NO^+ density reflected the conversion rate due to reaction (1) only. The effectiveness of the NO scavenger was estimated by assuming a rate coefficient for reaction (3) of at least $10^{-11} \text{ cm}^3/\text{sec}$ and values of the rate coefficient of reaction (2) from previous experiments. Experimentally, the effectiveness of the scavenger concentration was monitored by observing the disappearance of $\text{NO}^+ \text{N}_2$ in the ion mass spectrum upon addition of NO and also by noting that further increases of the NO concentration (up to 6% of N_2) had only a negligible effect on the rate of decline of the parent ions NO^+ .

The measured rate coefficients at temperatures between 100 K and 180 K and N_2 densities of typically $1 \times 10^{16} \text{ cm}^{-3}$ are shown in Fig. 1. Expressed in the functional form of a power law, the rate coefficient k_1 may be written as

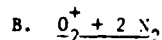
$$k_1 = (3 \pm 0.3) \times 10^{-31} (300/T)^{4.3} \text{ cm}^6/\text{sec} \quad (4)$$

where the coefficient were obtained by fitting to the present data only. It seems remarkable that an extrapolation of the present data to 300 K reproduces an independent determination of k_1 at 300 K by Heimerl and Vanderhoff (1974) quite well, as indicated in Fig. 1.

While the rate coefficient for thermal dissociation of $\text{NO}^+ \text{N}_2$ in N_2 , reaction (2), was not measured directly in this work, it may be inferred from previously measured equilibrium constants (Johnsen et al. 1975, Turner and Conway, 1976) $K = k_1/k_2$ and Eq. (4). With the equilibrium constants given by Johnsen et al. one obtains for k_2 :

$$k_2(T) = 1.5 \times 10^{-8} (300/T)^{4.3} \exp(-2093/T) \text{ cm}^3/\text{sec} \quad (5)$$

Calculated values for k_2 based on this expression are shown as a dashed line in Fig. 1.



In many respects the measurements of the association of O_2^+ ions with N_2



were quite similar to those of NO^+ . In order to circumvent the problem of thermal dissociation of $\text{O}_2^+ \text{N}_2$ ions, i.e. the reaction



typically 1.5-3.5% of oxygen were added to the nitrogen with the result that the switching reaction



quickly converted the $\text{O}_2^+ \text{N}_2$ ions into the more stable O_4^+ ions. By using varying admixtures of O_2 it was established that the measured rate coefficient for reaction (6) did not depend on the particular O_2 concentration chosen. The measured rate coefficients k_6 for reaction (6) are shown in Fig. 2 as a function of the gas temperature. The data in Fig. 2 may be fitted quite well by a power law of the form

$$k_6(T) = (1.0 \pm 0.1) \times 10^{-30} (300/T)^{3.2} \text{ cm}^6/\text{sec} \quad (9)$$

As indicated in Fig. 2, an extrapolation of the present data to 300 K using Eq. (9) agrees rather well with an independent measurement of k_6 by Howard et al. (1972). The temperature dependence of thermal dissociation of $\text{O}_2^+ \text{N}_2$ with N_2 may be inferred from Eq. (9) and the measured equilibrium constants of Janik and Conway (1976) for the inverse reactions (6) and (7). One obtains the expression:

$$k_7(T) = 1.7 \times 10^{-7} (300/T)^{3.2} \exp(-2676/T) \text{ cm}^3/\text{sec} \quad (10)$$

Values of k_7 calculated from this expression are also plotted in Fig. 2.

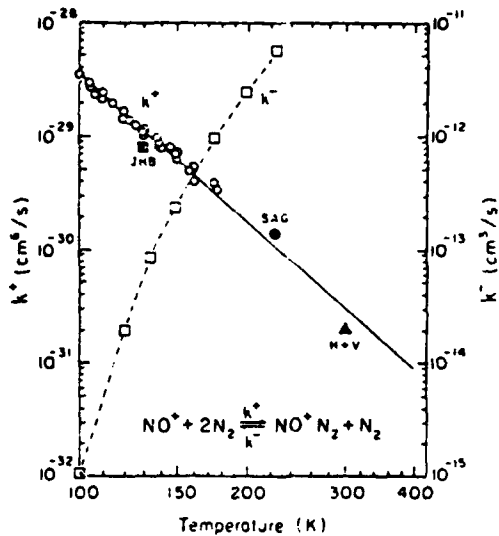
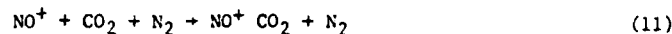


Fig. 1 Measured rate coefficients $k^+ = k_1$ for association of NO^+ ions in N_2 . Open circles: present data. Other data points marked H + V: Heimerl and Vanderhoff (1974), SAG: Smith et al. (1977), JHB: Johnsen et al. (1979). Open squares: inferred rate coefficients $k^- = k_2$ for thermal dissociation of $\text{NO}^+ \text{N}_2$. (Use right-hand scale to read values of k^- .)

C. $\text{NO}^+ + \text{CO}_2 + \text{N}_2$

At the temperatures used in the experiment the ion NO^+ - CO_2 was sufficiently stable against thermal dissociation to permit a direct measurement of the reaction rate of



without employing scavenger gases. Rate coefficients for this reaction were derived from the observed decay rates of NO^+ ions in N_2 - CO_2 mixtures in which the CO_2 admixture was typically from 5 to 20% of the N_2 concentration. Generally, the N_2 concentration was held constant and measurements were carried out at different CO_2 densities in order to obtain the increase of the effective rate coefficient with CO_2 addition. The quality of the data was somewhat poorer than that obtained in the other measurements because of the difficulty of keeping gas temperature and both gas concentrations constant for extended periods of time. The data points shown in Fig. 3 are possibly subject to errors on the order of 30% at the lower temperatures because of this difficulty. It seems unlikely though that the disagreement between the present data and those by Dunkin et al. (1971) and Smith et al. (1977) was caused by a systematic error in the present work. The temperature dependence of k_{11} based on fitting a power law to the data may be expressed as:

$$k_3 = (1.4 \pm 0.4) \times 10^{-29} (300/T)^{4.0} \text{ cm}^6/\text{sec} \quad (12)$$

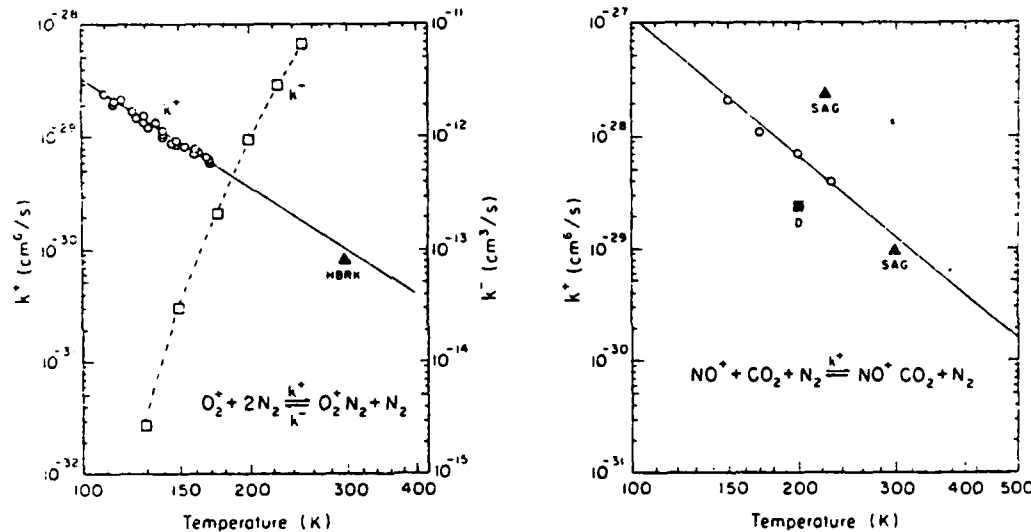


Fig. 2 Measured rate coefficients $k^+ = k_6$ for association of O_2^+ ions with N_2 . Open circles: present data. Point marked HBRK from Howard et al. (1972). Open squares: Inferred rate coefficients $k^- = k_7$ for thermal dissociation of O_2^+ - N_2 . (Use right-hand scale to read values of k^- .)

Fig. 3 Measured rate coefficients $k^+ = k_{11}$ for association of NO^+ ions in CO_2 with N_2 as third body. Open circles: Present data. Points marked SAG from Smith et al. (1977). Point marked D from Dunkin et al. (1971).

D. $\text{N}^+ + 2 \text{N}_2$ and $\text{N}_2^+ + 2 \text{N}_2$

Both N_3^+ and N_4^+ are stable against thermal dissociation at the temperatures used such that the forward rate coefficient of the reactions



and



could be measured over a wide range of temperatures without difficulty. Break-up of N_4^+ ions into $\text{N}_3^+ + \text{N}_2$ was observed, however, as a result of collisions with residual gas molecules in the transfer space between the drift chamber and the mass spectrometer. The N_3^+ ions resulting from collisional dissociation were distinguishable from those N_3^+ ions entering from the drift chamber by their different transit times (the ionic mobility of N_4^+ in N_2 is larger than that of N_3^+ by about 25%).

The measured rate coefficients for reaction (13) are shown in Fig. (4) as a function of gas temperature. The agreement of the present data obtained at 300 K with the drift tube measurements by Moseley et al. (1969) is seen to be excellent. The dependence of k_{13} on temperature is quite well described by the power law:

$$k_{13} = (2 \pm 0.2) \times 10^{-29} (300/T)^{2.0} \text{ cm}^6/\text{sec} \quad (15)$$

The results for reaction (14) are shown in Fig. 5 together with the 300 K measurements by Moseley et al. (1969) and the results obtained by Bohringer and Arnold (1982) at temperatures from 45 K to 400 K. There appears to be a systematic disagreement between the data by Bohringer and Arnold and the present data as well as the 300 K data by Moseley et al. of about 30% at 300 K. A further measurement (Meot-Ner and Field 1974) also yielded somewhat larger rate coefficients in the temperature range between 250 K and 500 K. The disagreements between different measurements in the case of this rather uncomplicated reaction indicate that unrecognized systematic errors are still present in some experimental techniques, but it is difficult to identify the problems.

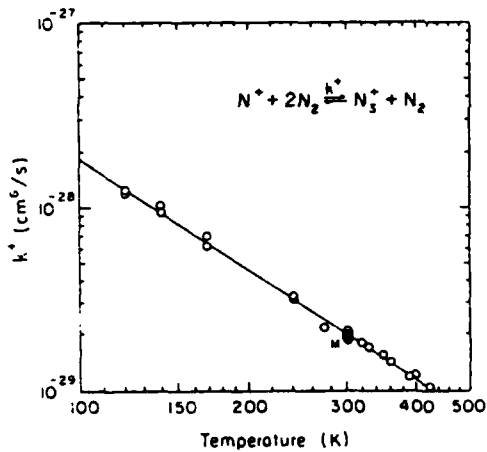


Fig. 4 Measured rate coefficients $k^+ = k_{13}$ for association of N^+ ions in N_2 . Open circles: Present data. Point marked M from Moseley et al. (1969).

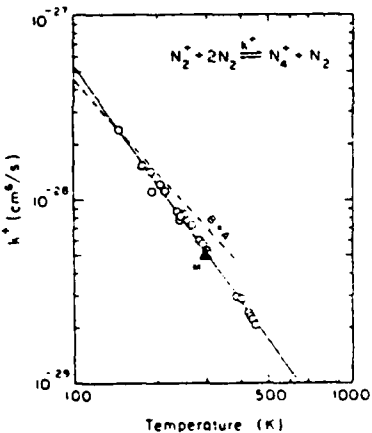


Fig. 5 Measured rate coefficients $k^+ = k_{14}$ for association of N_2^+ ions in N_2 . Open circles: Present data. Point marked M from Moseley et al. (1969). The dashed line marked B + A represents the data by Bohringer and Arnold (1982) as fitted by those authors.

A least-squares fit to the present data yields a temperature dependence of k_{14} in the form:

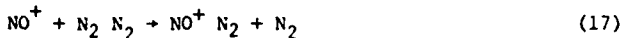
$$k_{14} = (5.0 \pm 0.5) \times 10^{-29} (300/T)^{2.14} \text{ cm}^6/\text{sec} \quad (16)$$

4. DISCUSSION OF RESULTS

As far as applications of the present results to D-region ion chemistry are concerned, the most important of the reactions studied is probably the association of NO^+ ions with N_2 , which is thought to be the first and rate limiting step in the NO^+ clustering sequence. The results presented here essentially confirm the conclusions drawn earlier (Johnsen et al. 1975) on the basis of incomplete experimental data. The measured rate coefficient exhibits the strong temperature dependence, $k \propto T^{-4.3}$, required by the model of Arnold et al. (1979), which yielded a T^{-5} dependence. Thus, it appears that the essential features of the model are correct.

The clustering of O_2 with N_2 is probably of lesser importance under normal D-region conditions, but it may play a role under disturbed conditions (Arnold et al. 1979). Quantitative model predictions for the temperature dependence of this reaction unfortunately are not available.

Approaching the problem from a distinctly different point of view, Calo and Narcisi (1980) recently proposed that the conventional three-body clustering mechanisms are deficient, since no allowance is made for reactions with neutral dimers, which should be present in the D-region and also in laboratory measurements. For instance, reactions of the type



could produce the same product ions as three-body association and, since the dimer concentration increases with the square of the N_2 density, the reaction would exhibit the same reaction order as a three-body reaction with an apparent rate coefficient $k^* = k_{17} K_{\text{equ.}}$, where $K_{\text{equ.}} = [\text{N}_2 \text{N}_2] / [\text{N}_2]^2$.

From the theory of Stogryn and Hirschfelder (1959), Calo and Narcisi obtained $K_{\text{equ.}} = 7.6 \times 10^{-23} \text{ cm}^3$ at $T = 187 \text{ K}$. (Due to a typographical error the number given in that article is too small by a factor of ten. Narcisi, private communication). Assuming that $k_{17} = 10^{-9} \text{ cm}^3/\text{sec}$ one obtains $k^* = 7.6 \times 10^{-32} \text{ cm}^6/\text{sec}$, which is only 3.8 % of the measured value for k_1 at 187 K. The higher estimates for the dimer contribution given by Calo and Narcisi are due to their assumption of a smaller value for k_1 . Furthermore, the estimates for $K_{\text{equ.}}$ are based on the free-rotor model of N_2 molecules in the dimer, which appears to give dimer concentrations 100 times larger than observed experimentally (Leckenby and Robbins, 1965). In conclusion, it seems that dimerization of N_2 has only a negligible effect at D-region temperatures and that laboratory measurements yield actual rather than apparent three-body association coefficients.

ACKNOWLEDGEMENTS

This research was supported, in part, by the Defense Nuclear Agency (monitored by the Air Force Geophysics Laboratory) under Contract No. F19628-81-K-0002.

REFERENCES

Arnold, F., Krankowsky, D., Zettwitz, E., and Joos, W. (1979). *J. Atm. and Terr. Phys.* **42**, 249-256.
 Bohringer, H. and Arnold, F. (1982). *J. Chem. Phys.* **77**, 5534-5541.
 Calo, J. M. and Narcisi, R. S. (1980). *Geophys. Res. Lett.* **7**, 289-292.
 Dunkin, D. B., Fehsenfeld, F. C., Schmeltekopf, A. L., and Ferguson, E. E. (1971). *J. Chem. Phys.* **54**, 3817-3822.
 Heimerl, J. M. and Vänderhoff, J. A. (1974). *J. Chem. Phys.* **60**, 4362-4368.
 Howard, C. J., Bierbaum, V. M., Rundle, H. W., and Kaufman, F. (1972). *J. Chem. Phys.* **57**, 3491.
 Janik, G. S. and Conway, D. C. (1976). *J. Phys. Chem.* **71**, 823-829.
 Johnsen, R., Huang, C. M., and Biondi, M. A. (1975). *J. Chem. Phys.* **63**, 3374-3378.
 Johnsen, R., Chen, A., and Biondi, M. A. (1979). *J. Chem. Phys.* **72**, 3085-3088.
 Leckenby, R. E. and Robbins, E. J. (1965). *Proc. Roy. Soc.* **291 A**, 389-412.
 Moseley, M. and Field, F. H. (1974). *J. Chem. Phys.* **61**, 3742-3749.
 Moseley, J. T., Snuggs, R. M., Martin, D. W., and McDaniel, E. W. (1969). *Phys. Rev.* **178**, 240-248.
 Smith, D., Adams, N. G., and Grief, D. (1977). *J. of Atm. and Terr. Phys.* **39**, 513-521.
 Stogryn, D. E. and Hirschfelder, J. O. (1959). *J. Chem. Phys.* **31**, 1531-1545.
 Turner, D. L. and Conway, D. C. (1976). *J. Chem. Phys.* **65**, 3947-3947.

Electron-temperature dependence of dissociative recombination of electrons with $\text{CO}^+ \cdot (\text{CO})_n^-$ series ions

Marlin Whitaker, Manfred A. Biondi, and Rainer Johnsen

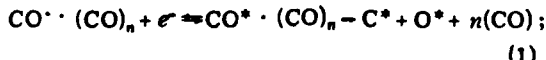
Department of Physics and Astronomy, University of Pittsburgh, Pittsburgh, Pennsylvania 15260

(Received 29 September 1980)

A microwave-afterglow mass-spectrometer apparatus has been used to determine the dependence on electron temperature T_e of the recombination coefficients α_n of the dimer and trimer ions of the series $\text{CO}^+ \cdot (\text{CO})_n^-$. We find $\alpha_1 = (1.3 \pm 0.3) \times 10^{-6} [T_e(\text{K})/300]^{-0.14}$ and $\alpha_2 = (1.9 \pm 0.4) \times 10^{-6} [T_e(\text{K})/300]^{-0.13} \text{ cm}^3/\text{sec}$. These dependences on T_e are quite different from those obtained previously for polar-cluster ions of the hydronium and ammonium series but are similar to that for simple diatomic ions.

I. INTRODUCTION

The capture of electrons by ions of the carbon monoxide series, $\text{CO}^+ \cdot (\text{CO})_n^-$, where $n = 0, 1, 2, \dots$, is of interest for several reasons. These ions may be important in ionized media where CO or CO_2 are among the neutral constituents, as in some laser plasmas or in the ionospheres of certain planetary atmospheres. Thus, determinations of the electron-ion recombination coefficients for the appropriate ions provide needed inputs to model calculations of the behavior of these plasmas. More fundamentally, previous studies¹⁻³ have shown that recombination coefficients for ions to which strongly polar molecules are clustered exhibit a very different variation with electron temperature than that observed for dissociative recombination of unclustered molecular ions.⁴ The present study extends the cluster-ion work by examining recombination of ions clustered with weakly polar molecules, i.e., the dimer and trimer ions, $\text{CO}^+ \cdot \text{CO}$ and $\text{CO}^+ \cdot (\text{CO})_2$, where the recombination reaction is most probably



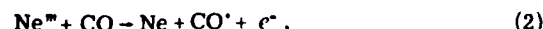
the asterisks indicate that the products may be electronically excited.

II. METHOD OF MEASUREMENT AND DATA ANALYSIS

The microwave-afterglow mass-spectrometer apparatus is the same as that used previously in a study of the polar-cluster ions⁵ and has been described in some detail.⁵ A microwave discharge lasting typically 0.1 msec and repeated at a 10-Hz rate is generated in 5–20 Torr of neon containing an admixture of a few tenths percent of carbon monoxide. The “microwave-averaged” electron density \bar{n}_{ee} during the afterglow is obtained from measurements of the resonant-frequency shift of the high- Q TM_{010} cavity mode,¹ while steady elec-

tron heating is achieved by application of microwave power via a low- Q (~ 10) TE_{111} cavity mode. The time histories of the various afterglow ions are determined by sampling the ions which diffuse to the cavity wall and effuse through a small orifice into a differentially pumped quadrupole mass filter.

The principal steps in the formation of the ions of interest are thought to be (a) electron-impact excitation of neon to a metastable state Ne^m , (b) Penning ionization of CO molecules via



and (c) clustering and breakup reactions,



and



The relative abundance of ions in the afterglow is controlled by varying the gas temperature from ~ 250 to 300 K and the partial pressure of CO from ~ 20 to 100 mTorr, thereby affecting the equilibria of reactions (3) and (4). (Under the conditions of the present measurements the CO^+ ion was never a significant ion throughout the afterglow, so that its recombination coefficient was not determined.)

Under the conditions obtaining in the present study, that is, the ions present in significant concentrations decay together during the afterglow, it has been shown³ that the electron continuity equation can be written as

$$\frac{\partial n_e(r, t)}{\partial t} \approx -\sigma_{\text{eff}} n_e^2 + D_e \nabla^2 n_e, \quad (5)$$

where σ_{eff} , the effective recombination coefficient, is given by $\sigma_{\text{eff}} = \sum \sigma_i f_i$, in which the f_i are the fractional concentrations (essentially time independent) of each afterglow ion and D_e is the ambipolar diffusion coefficient appropriate to a mixture of positive ions,⁶ whose separate D_e values are

estimated from the Langevin (polarization) mobilities⁷ of ions moving in neon. Usually only two ionic species are present in significant concentrations during the afterglow (e.g., the dimer and trimer ions); therefore α_{eff} may be written as

$$\alpha_{\text{eff}} = f_1 \alpha_1 + (1 - f_1) \alpha_2, \quad (6)$$

with α_1 the dimer- and α_2 the trimer-ion recombination coefficients.

A computer solution^{8,9} of Eq. (5) with appropriate values of α_{eff} and D_e yields the predicted spatial and temporal variation of the electron density, from which predicted values of $\bar{n}_{\mu\mu}$ (t) can be obtained. Since the measurements of the microwave cavity's resonant-frequency shift during the afterglow directly yield $\bar{n}_{\mu\mu}$ (t), the value of α_{eff} may be determined from these measurements by obtaining a best fit to the data of computer-generated solutions of Eq. (5), using the known values of D_e and treating α_{eff} as a parameter.

III. RESULTS

A number of attempts were made to achieve conditions in which CO^+ ions were the principal afterglow ions, however, without success. Consequently, we were unable to determine the recombination coefficient for the CO^+ monomer ion.

The recombination coefficient for the dimer ion, $\text{CO}^+ \cdot \text{CO}$, was inferred from those data runs in which the dimer was the only ion of significance,

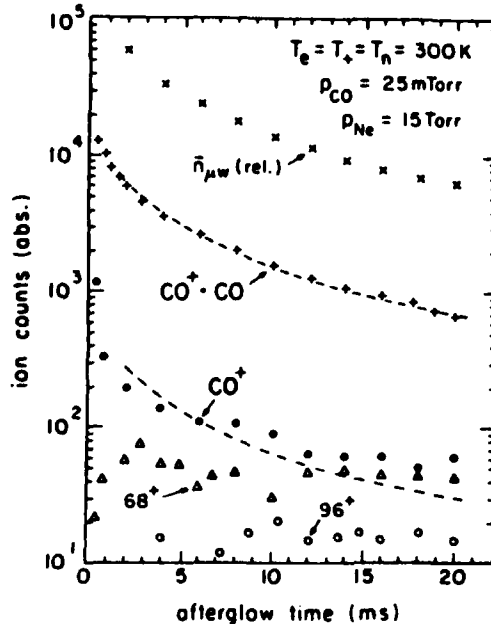


FIG. 1. Comparative decays of volume electron density $\bar{n}_{\mu\mu}$ and ion wall currents during the afterglow. The dashed lines represent renormalized values of $\bar{n}_{\mu\mu}$.

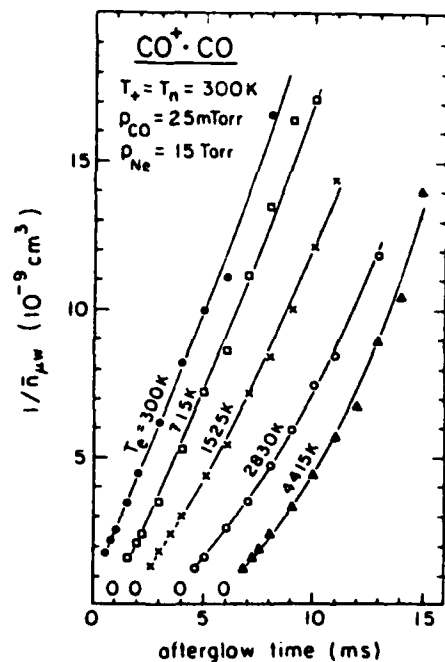


FIG. 2. $1/\bar{n}_{\mu\mu}$ vs time "recombination decay" plots for various electron temperatures under the same conditions as Fig. 1. The solid lines represent best-fit computer solutions of Eq. (5) to the data. The zero times for the different T_e runs are displaced for clarity.

representing greater than 90% of the total ion count. Referring to Fig. 1, it will be seen that in this example of our measurements the electron density decay tracks the $\text{CO}^+ \cdot \text{CO}$ wall current decay (the dashed lines are renormalized $\bar{n}_{\mu\mu}$ values) and that the CO^+ concentration is <5% of the dimer ion concentration during the ~12 msec of the after-

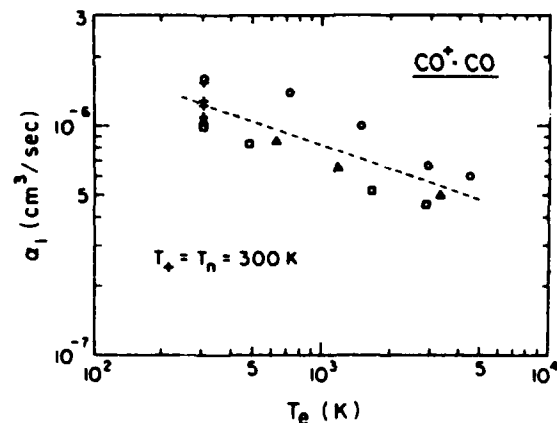


FIG. 3. Variation with electron temperature of the dimer-ion recombination coefficient with $T_e = T_n = 300$ K. Each type of symbol indicates a run taken with a given gas filling on a given day. The dashed line represents a $T_e^{-0.34}$ power-law dependence for α_1 .

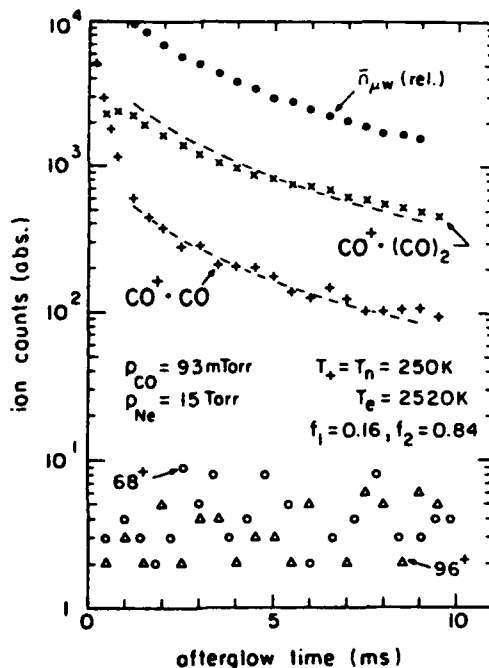


FIG. 4. Comparative decays of $\bar{n}_{\mu w}$ and ion wall currents in an afterglow in which trimer and dimer ions are the principal positive ions.

glow used to determine α . Figure 2 shows examples of the measured electron-density decays for several electron temperatures displayed in the "recombination-decay" form of $1/\bar{n}_{\mu w}$ vs. t . The solid lines are computer solutions of Eq. (5) which provide the best fit to the data. The measured variation with electron temperature for α for the dimer ions is shown in Fig. 3. The different symbols (circles, triangles, squares) indicate separate sequences of runs taken some days apart and suggest that the T_e variation from one run to the next is more reproducible than is the absolute value of $\alpha[\text{CO}^+ \cdot \text{CO}]$ at a given value of T_e . The + symbols indicate the reproducibility of α values determined from several runs all at $T_e = 300$ K.

In those runs where the trimer ion, $\text{CO}^+ \cdot (\text{CO})_2$, was dominant, it was necessary in many cases to correct for the presence of significant fractions of the dimer ion. An example of the tracking of the electron density decay with the decays of the trimer and dimer ions is given in Fig. 4. Electron density decays measured at various electron temperatures for the case where both trimer (at 84%) and dimer (at 16%) ions were present are shown in Fig. 5. The solid lines represent best-fits of the computer solutions of Eq. (5) to the data to obtain α_{eff} vs. T_e . When the α_{eff} data were corrected via Eq. (6) for the dimer-ion contribution using the appropriate values of α_1 , the inferred

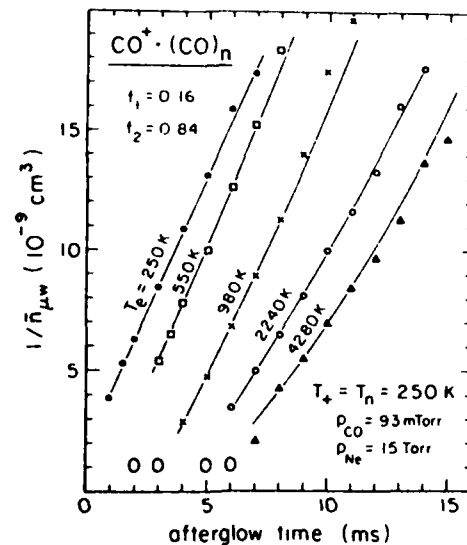


FIG. 5. $1/\bar{n}_{\mu w}$ vs time curves for the same conditions as Fig. 4. The solid lines are best-fit computer solutions of Eq. (5) to the data. The zero times of successive runs are displaced for clarity.

variation of the trimer-ion recombination coefficient α_2 with T_e shown in Fig. 6 was obtained. Again the different symbols represent different runs.

If one fits the data of Figs. 3 and 6 to simple power-law variations of the form $\alpha \sim T_e^x$, the results of the studies can be represented by the following expressions:

$$\alpha[\text{CO}^+ \cdot \text{CO}](\text{cm}^3/\text{sec}) = (1.3 \pm 0.3) \times 10^{-6} [T_e(\text{K})/300]^{-0.34} \quad (7)$$

and

$$\alpha[\text{CO}^+ \cdot (\text{CO})_2](\text{cm}^3/\text{sec}) = (1.9 \pm 0.4) \times 10^{-6} [T_e(\text{K})/300]^{-0.33}, \quad (8)$$

where the stated uncertainties reflect our estimates of the systematic and random errors associated with the determinations. While the data of Fig. 3 show no systematic deviation from the expression given in Eq. (7), the data of Fig. 6 suggest that initially $\alpha[\text{CO}^+ \cdot (\text{CO})_2]$ may decrease more slowly with increasing T_e than the expression of Eq. (8) suggests and then, above 1000 K, more rapidly.

IV. DISCUSSION AND CONCLUSIONS

The present studies of recombination of electrons with the carbon monoxide family of cluster ions indicate a dependence of the recombination coefficient on electron temperature which is quite like that found for unclustered molecular ions. This

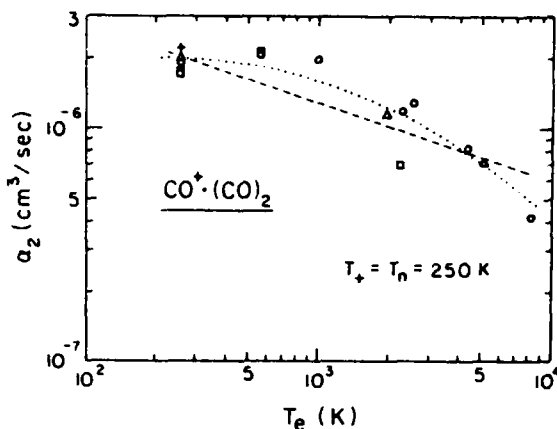


FIG. 6. Variation of the trimer-ion recombination coefficient with T_e for $T_e = T_n = 250$ K. While the dashed line represents a power-law variation of the form $\alpha_2 \sim T_e^{-0.33}$, the dotted line may better represent the actual variation.

result is in sharp contrast to the virtually electron-temperature-independent recombination exhibited by the clustered ions of the ammonium² and hydronium³ series. Thus, the dimer and trimer ions of the $\text{CO}^+ \cdot (\text{CO})_n$ series exhibit some properties of both unclustered and polar-cluster molecular ions; i.e., they have large coefficients at $T_e \sim 300$ K (somewhat greater than $10^{-6} \text{ cm}^3/\text{sec}$), as do comparably clustered $\text{NH}_4^+ \cdot (\text{NH}_4)_n$ and $\text{H}_3\text{O}^+ \cdot (\text{H}_2\text{O})_n$ series ions; however, the dependence of α on T_e approaches that predicted ($T_e^{1/2}$) and observed ($\sim T_e^{0.4}$ to $T_e^{0.6}$) for the direct dissociative process for simple diatomic ions.⁴

The substantially larger α values for the dimer and trimer ions compared to that expected¹⁰ for the monomer ion CO^+ probably result from the increased likelihood of electron capture via an inelastic energy loss to the complex during the initial Coulomb collision. If the probability of such inelastic losses varies slowly with electron energy owing to the many closely spaced rotational and vibrational levels in the complex, then the Coulomb cross section's $1/\epsilon$ energy variation (ϵ is the electron energy) dominates the capture. If, in addition, the stabilization by dissociation of the core [refer to reaction (1)] is highly probable, one then expects a variation of α near $T_e^{1/2}$. Although this argument makes plausible the $\text{CO}^+ \cdot (\text{CO})_n$ data, it appears that a similar argument should apply to the hydronium and ammonium series ions. Thus, the observed lack of dependence of α on T_e in the latter cases^{2,3} is difficult to understand.

Earlier studies¹¹⁻¹³ of electron-ion recombination

in CO discharge afterglows did not employ mass identification of the recombining ions. Thus, the attribution of a measured recombination loss rate to a particular ionic species in such studies is, in our view, rather speculative.

Mentzoni and Donohue interpreted the lack of a pressure dependence over the range $0.2 \leq p(\text{CO}) \leq 2$ Torr in their recombination coefficient determinations¹² as evidence that CO^+ was the dominant afterglow ion, concluding that $\alpha[\text{CO}^+] \approx 4 \times 10^{-7} \text{ cm}^3/\text{sec}$ at $T_e = 775$ K. In their earlier work¹¹ they found a constant value, $\alpha \approx 7 \times 10^{-7} \text{ cm}^3/\text{sec}$, even when the electron temperature was decaying to $T_e = 300$ K during the afterglow; however, in their second paper¹² they use this value for $T_e = 300$ K and, on the basis of these two T_e values, infer a $T_e^{-0.6}$ dependence for $\alpha[\text{CO}^+]$. While this T_e dependence is reasonable, the absolute value appears to be about a factor of 2, too high,¹⁰ and may result from the presence of dimer or trimer ions along with the CO^+ monomer. Our mass analysis of ions in discharge afterglows in CO-Ne mixtures indicates the presence of a mixture of ions, e.g., CO^+ , CO^+ , CO , and C_nO_m^+ , at CO pressures above 0.1 Torr.

As noted in Sec. III, we made substantial efforts to determine $\alpha(\text{CO}^+)$ but were unable to achieve conditions in the CO-Ne discharge afterglows where CO^+ was the dominant afterglow ion. For CO partial pressures below ~ 1 mTorr, both neon ions from the buffer gas and impurity ions as well as CO^+ ions were present, complicating analysis of the electron density decays, while for $p(\text{CO}) > 3$ mTorr, dimer or more complex ions were dominant.

Center¹³ studied electron loss by recombination in high-pressure afterglows ($100 \leq p(\text{CO}) \leq 700$ Torr) where cluster ions were almost certainly present (as he noted). His values of "a" for the unknown ionic mixture are comparable to our values for the dimer or trimer ions at $T_e \sim 1000$ K but decrease much more rapidly with increasing T_e , differing from our results by a factor ~ 3 at $T_e \sim 5000$ K. In our view, this discrepancy points out the difficulty of making quantitative determinations of recombination coefficients for specified ions in molecular gases in the absence of ionic mass identification.

ACKNOWLEDGMENTS

This research was supported, in part, by the NASA Planetary Atmospheres Program under Grant No. NGL-39-011-137 and the U.S. Army Research Office/DNA under Grant No. DAAG-29-80-C-0075.

¹M. T. Leu, M. A. Biondi, and R. Johnsen, *Phys. Rev. A* 7, 292 (1973).

²C. M. Huang, M. A. Biondi, and R. Johnsen, *Phys. Rev. A* 14, 984 (1976).

³C. M. Huang, M. Whitaker, M. A. Biondi, and R. Johnsen, *Phys. Rev. A* 18, 64 (1978).

⁴J. N. Bardsley and M. A. Biondi, in *Advances in Atomic and Molecular Physics*, edited by D. R. Bates (Academic, New York, 1970), Vol. 6.

⁵F. J. Mehr and M. A. Biondi, *Phys. Rev.* 181, 264 (1969).

⁶A. V. Phelps and S. C. Brown, *Phys. Rev.* 86, 102 (1952).

⁷P. Langevin, *Ann. Chim. Phys.* 5, 245 (1905).

⁸L. Frommhold and M. A. Biondi, *Ann. Phys.* 48, 107 (1968).

⁹L. Frommhold, M. A. Biondi, and F. J. Mehr, *Phys. Rev.* 165, 44 (1968).

¹⁰M. A. Biondi, *Comments At. Mol. Phys.* 4, 85 (1973).

¹¹M. H. Mentzoni and J. Donohoe, *Phys. Lett.* 26A, 330 (1968).

¹²M. H. Mentzoni and J. Donohoe, *Can. J. Phys.* 47, 1789 (1969).

¹³R. E. Center, *J. Appl. Phys.* 44, 3538 (1973).

Electron-temperature dependence of dissociative recombination of electrons with $N_2^+ \cdot N_2$ dimer ions

Marlin Whitaker, Mansfred A. Biondi, and Rainer Johnsen

Department of Physics and Astronomy, University of Pittsburgh, Pittsburgh, Pennsylvania 15260

(Received 16 March 1981)

A microwave-afterglow mass-spectrometer apparatus has been used to determine the dependence on electron temperature T_e of the recombination coefficient of electrons with the dimer ion $N_2^+ \cdot N_2$. We find $\alpha = (1.4 \pm 0.2) \times 10^{-6} [T_e (K)/300]^{0.41} \text{ cm}^3/\text{s}$ over the range $300 \leq T_e \leq 5600 \text{ K}$, and $T_e = T_n = T_s = 300 \text{ K}$. These results are quite similar to those found for the $CO^+ \cdot CO$ dimer ion but quite different from the T_e^{-1} dependence inferred from previous measurements in nitrogen in which the ions were not mass identified.

I. INTRODUCTION

The present study of the variation with electron temperature T_e of the dissociative recombination of electrons with $N_2^+ \cdot N_2$ dimer ions was undertaken to extend our recent investigations¹ of the mechanism of dimer-ion recombination and to provide needed data for modeling lower-ionspheric regions and high-pressure laser plasmas where such ions might be expected. While the variation with T_e of the dissociative recombination coefficient α for simple diatomic ions has been found² to approximate the $T_e^{-1/2}$ dependence predicted theoretically for relatively simple diatomic ions, recombination coefficients for cluster ions containing strongly polar molecules, e.g., $H_3O^+ \cdot H_2O$ and $NH_4^+ \cdot NH_3$, exhibit^{3,4} a very weak variation, approaching T_e^0 .

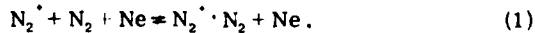
A fast dissociative process is expected to be largely controlled by the initial Coulomb-collision capture step whose cross section σ_{cap} varies as $1/e$ (e is the electron energy) leading to a $\sim T_e^{-1/2}$ variation of $\alpha = \langle \sigma v_e \rangle$, where v_e is the electron velocity and the angular brackets indicate averaging over the velocity distribution. Thus, the finding¹ of a $T_e^{-0.34}$ variation of α for the case of the dimer cluster ion ($CO^+ \cdot CO$) seemed quite reasonable, in contrast to the hydronium and ammonium cluster ion results.^{3,4} However, for the case of the dimer ion ($N_2^+ \cdot N_2$), an earlier inference⁵ of a T_e^{-1} dependence (for $T = T_n = T_s = T_e$) from studies without mass identification of the ions was difficult to understand, motivating us to reinvestigate this dimer ion with an apparatus providing positive identification of the ions under study.

II. METHOD OF MEASUREMENT AND DATA ANALYSIS

The microwave-afterglow mass-spectrometer apparatus and method of measurement have been

described in detail previously.⁶ A microwave discharge lasting typically 1 ms and repeated at a 10-Hz rate is generated in mixtures of ~ 10 –100 mTorr of nitrogen and ~ 8 –20 Torr of neon. The decay curves of the various afterglow ions are determined by sampling the ions which diffuse to the cavity wall and effuse through a small orifice into a differentially pumped quadrupole mass filter. The "microwave-averaged" electron density $\bar{n}_{\mu m}$ during the afterglow is obtained from measurements of the resonant-frequency shift of the high- Q TM_{010} cavity mode, while steady electron heating is achieved by application of microwave power via a low- Q TE_{111} cavity mode. Since, as discussed in an earlier paper,⁷ the heating microwave electric field produces an essentially Maxwellian electron velocity distribution,⁸ it is appropriate to use the electron temperature T_e to characterize the elevated electron mean energy.

The principal steps in the formation of the nitrogen dimer ion are thought to be the following: (a) electron-impact excitation of neon to a metastable state Ne^m , (b) Penning ionization via $Ne^m + N_2 \rightarrow Ne + N_2 + e^-$, and (c) the clustering and breakup reaction



The relative abundance of ions in the afterglow is controlled by varying the partial pressure of N_2 , thereby affecting the equilibrium of reaction (1).

For the case in which only one ion is present in an afterglow dominated by electron-ion recombination and ambipolar diffusion loss, the continuity equation for the electrons is given by⁶

$$\frac{\partial n_e}{\partial t} \approx -\alpha n_e^2 + D_a \nabla^2 n_e, \quad (2)$$

where D_a is the ambipolar diffusion coefficient. A point-by-point computer solution⁹ of Eq. (2)

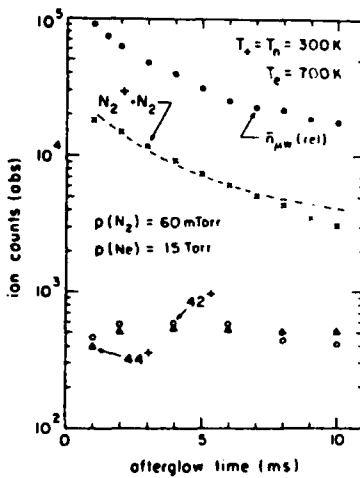


FIG. 1. Comparative decays of volume electron density \bar{n}_{μ_w} and ion wall current during the afterglow. The dashed line represents renormalized values of \bar{n}_{μ_w} .

yields the predicted spatial and temporal variation of the electron density, $n_e(\mathbf{r}, t)$, from which values of $\bar{n}_{\mu_w}(t)$ may be computed.

The measurements of the microwave cavity's resonant-frequency shift during the afterglow yield directly the values of the microwave-averaged electron density $\bar{n}_{\mu_w}(t)$.⁶ The value of the recombination coefficient α is determined by obtaining a best fit to the \bar{n}_{μ_w} data of the computer-generated solutions of Eq. (2), using values of D_e for N_4^+ ions in Ne calculated from the Langevin polarization interaction formula¹⁰ (empirically increased by -25% to match data for other ions in neon) and treating α as a parameter.

III. RESULTS

The recombination coefficient of the $\text{N}_2^+ \cdot \text{N}_2$ ion was determined from those runs in which the dimer was the only ion of significance in the afterglow, thereby allowing us to employ the simple analysis described above. An example of the measured decays of electron density and ion wall currents is given in Fig. 1. The ion $\text{N}_2^+ \cdot \text{N}_2$ is dominant, with small amounts (~5%) of 42⁺ ($\text{N}^+ \cdot \text{N}_2$) and 44⁺ (probably N_2O^+) the only other detectable ions. In addition, the $\text{N}_2^+ \cdot \text{N}_2$ ion wall current "tracks" the electron density reasonably well throughout the afterglow (the dashed line represents the \bar{n}_{μ_w} curve normalized to the $\text{N}_2^+ \cdot \text{N}_2$ data at 5 ms). The slight deviation at 8–10 ms probably reflects the increasing importance of the $\text{N}^+ \cdot \text{N}_2$ and N_2O^+ ions in the late afterglow, since, if one compares \bar{n}_{μ_w} to the total ion count, the tracking is improved.

The variation of the electron density decays with

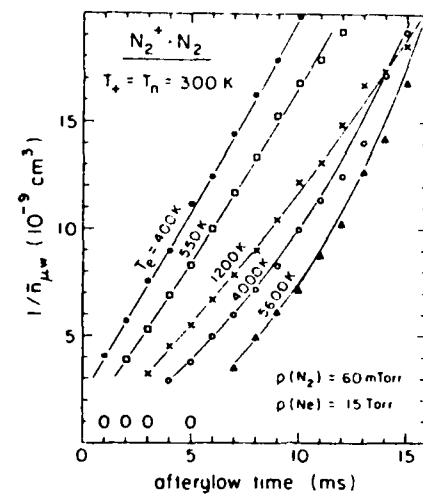


FIG. 2. "Recombination decay" plots of $1/\bar{n}_{\mu_w}$ vs time for various electron temperatures. The solid lines represent best-fit computer solutions of Eq. (2) to the data. The zero times for the different T_e runs are displaced for clarity.

electron temperature T_e is illustrated in Fig. 2. The zero time for the different T_e runs has been displaced for clarity. The solid lines through the data points are the computer solutions of Eq. (2) which provided a best fit to the data. The α values inferred from these fits to the data yield the variation of the recombination coefficient with electron temperature. The results of these and our other measurements are summarized in the plot of $\alpha(\text{N}_2^+ \cdot \text{N}_2)$ vs T_e given in Fig. 3. The extent of the bar symbols indicates our estimates of possible systematic and random errors in the determinations.

A least-squares fit of the experimental data to a simple power-law dependence of the form $\alpha \sim T_e^{-x}$ yields the result indicated by the dashed line in Fig. 3 and given by the expression

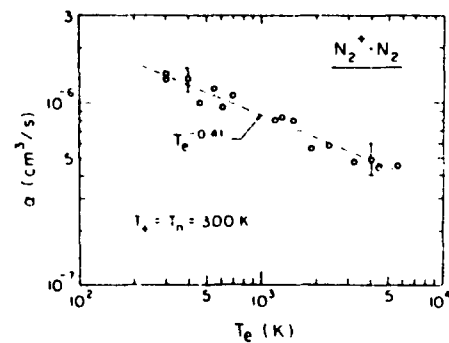


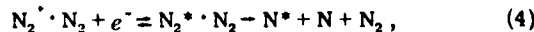
FIG. 3. Variation with electron temperature T_e of the dimer-ion recombination coefficient α . The dashed line represents a least-squares fit to the data of a simple power-law dependence, $\alpha \sim T_e^{-x}$, yielding $x = 0.41$.

$$\alpha(N_2^+ \cdot N_2) \text{ (cm}^3/\text{s}) = (1.4 \pm 0.2) \times 10^{-6} [T_e(\text{K})/300]^{-0.41}, \quad (3)$$

valid over the measured range $300 \leq T_e \leq 5600$ K. The data show no significant systematic deviations from the simple law.

IV. DISCUSSION AND CONCLUSIONS

The measured T_e variation, $\alpha(N_2^+ \cdot N_2) \sim T_e^{-0.41}$, for the nitrogen dimer ion is similar to that observed in our recent study¹ of the carbon monoxide dimer ion, $\alpha(CO^+ \cdot CO) \sim T_e^{-0.34}$, and is consistent with the expected energy dependence $\sim T_e^{-1/2}$ for a fast dissociative process, as discussed in the Introduction. The recombination may well involve a process of the form



that is, dissociation of the neutralized "core" ion together with detachment of the previously clustered neutral molecule.

Thus, the dimer ions of both nitrogen and carbon monoxide, involving a nonpolar or a weakly polar molecule clustered to the ion core do not exhibit the very feeble dependence of α on electron temperature noted for the $H_3O^+ \cdot H_2O$ and $NH_4^+ \cdot NH_3$ dimerlike cluster ions formed with

strongly polar molecules. At present we have no satisfactory explanation, in terms of the recombination mechanism, of the "pathological" behavior of the hydronium and ammonium-series cluster ions.

The measured $T_e^{-0.41}$ dependence for $\alpha(N_2^+ \cdot N_2)$ is much weaker than the $\sim T_e^{-1}$ dependence inferred earlier⁵ by combining data from two experiments, one involving an afterglow measurement at 300 K of mass-identified $N_2^+ \cdot N_2$ ions,¹¹ the other an afterglow measurement of the temperature dependence of α over the range 300–600 K (with $T_e = T_+ = T_n$) for an unknown mixture of ions in nitrogen at relatively high pressures (> 10 Torr).¹² In our view, the results of the present experiment, in which the identity of the ions undergoing recombination with the electrons is determined, should take precedence over the earlier results.

ACKNOWLEDGMENTS

This research was supported in part by the Defense Nuclear Agency (monitored by the Air Force Geophysics Laboratory) under Contract No. F19628-81-K-0002 and by the NASA Planetary Atmospheres Program under Grant No. NGL39-011-137.

¹M. Whitaker, M. A. Biondi, and R. Johnsen, *Phys. Rev. A* **23**, 1481 (1981).

²M. A. Biondi, in *Principles of Laser Plasmas*, edited by G. Bekefi (Wiley, New York, 1976), p. 137.

³C. M. Huang, M. Whitaker, M. A. Biondi, and R. Johnsen, *Phys. Rev. A* **19**, 64 (1978).

⁴C. M. Huang, M. A. Biondi, and R. Johnsen, *Phys. Rev. A* **14**, 984 (1976).

⁵M. A. Biondi, in *Reaction Rate Handbook*, 2nd ed., DNA 1948II, edited by M. H. Bortner and T. Bauer (Defense Nuclear Agency, Washington, D. C., 1978), pp. 16–10.

⁶F. J. Mehr and M. A. Biondi, *Phys. Rev.* **181**, 264 (1969).

⁷L. Frommhold, M. A. Biondi, and F. J. Mehr, *Phys. Rev.* **165**, 44 (1968).

⁸H. Margenau, *Phys. Rev.* **69**, 508 (1946).

⁹L. Frommhold and M. A. Biondi, *Ann. Phys. (N.Y.)* **48**, 407 (1968).

¹⁰P. Langevin, *Ann. Chim. Phys.* **5**, 245 (1905).

¹¹W. H. Kasner and M. A. Biondi, *Phys. Rev.* **137**, A317 (1965).

¹²R. Hackam, *Planet. Space Sci.* **13**, 667 (1965).

RECORDED

FILMED

PRINTED